

Striped antiferromagnetic order and electronic properties of stoichiometric LiFeAs from first-principles calculations

Yong-Feng Li and Bang-Gui Liu^a

Institute of Physics, Chinese Academy of Sciences, Beijing 100190, China
Beijing National Laboratory for Condensed Matter Physics, Beijing 100190, China

the date of receipt and acceptance should be inserted later

Abstract. We use state-of-the-arts first-principles method to investigate the structural, electronic, and magnetic properties of stoichiometric LiFeAs . We optimize fully all the structures, including lattice constants and internal position parameters, for different magnetic orders. We find the magnetic ground state by comparing the total energies among all the possible magnetic orders. Our calculated lattice constants and As internal position are in good agreement with experiment. The experimental fact that no magnetic phase transition has been observed at finite temperature can be attributed to the tiny inter-layer spin coupling. Our results show that stoichiometric LiFeAs has almost the same striped antiferromagnetic spin order as other FeAs-based parent compounds and tetragonal FeSe do, which may imply that all Fe-based superconductors have the same mechanism of superconductivity.

PACS. 75.10.-b General theory and models of magnetic ordering, 74.20.-z Theories and models of superconducting state, and 75.30.-m Intrinsic properties of magnetically ordered materials

1 Introduction

Since the discovery of superconductivity in F-doped LaFeAsO [1], many Fe-based superconductors have been achieved by doping appropriate atoms in or applying pressure on ROFeAs (R: rare earth) [2,3,4], AFe_2As_2 (A: alkaline earth) [5,6,7,8], SrFeAsF [9,10,11,12], LiFeAs [13,14,15,8], and even FeSe [16,17,18,19]. The highest transition temperature T_c has already reached to 55–56 K [4]. Various studies have been performed to understand their magnetic orders, electronic structures, superconductivity, etc [20,21,22,23,24,25,26,27]. Among the few series of Fe-based superconductors, the LiFeAs series seems to be the simplest FeAs-based superconductors. Many experiments have been done to promote T_c [29,13,30,15,14,28,31,32,33]. It should be easier to detect the mechanism of the superconductivity in this series. Although there have been some computational studies on LiFeAs [8,34,27], many aspects, even the magnetic properties of stoichiometric LiFeAs , are not elucidated. It is highly desirable to solve such basic issues of LiFeAs for further investigations and future applications of the FeAs-based materials.

Here, we investigate the structural, electronic, and magnetic properties of stoichiometric LiFeAs by using state-of-the-arts first-principles calculations. We compare all the possible magnetic orders, and find the magnetic ground state in terms of total energy results and force optimization. Our results show the magnetic ground state features

a striped antiferromagnetic (SAF) order in the Fe layer and a weak antiferromagnetic (AFM) order in the z direction perpendicular to the Fe layer. Our calculated internal positions of Li and As are in good agreement with experiment. Through analyzing electronic and the magnetic results, we propose a simple spin model to understand the experimental magnetic properties. Thus, we show that stoichiometric LiFeAs has almost the same SAF spin order as other FeAs-based parent compounds and tetragonal FeSe do. More detailed results will be presented in the following.

In next section we shall describe our computational details. In the third section we shall optimize fully all the structures with different magnetic orders and thus determine the magnetic ground state. In the fourth section we shall present the electronic structures of the ground state phase. Finally, we shall make some discussions and give our conclusion in the fifth section.

2 Computational details

We investigate all possible magnetic orders for stoichiometric LiFeAs by using full-potential linearized augmented plane wave method within the density functional theory [35], as implemented in package WIEN2k [36,37]. The generalized gradient approximation is used for the exchange and correlation potentials [38]. We treat Li-2s, Fe-3d4s, and As-4s4p as valence states, Fe-3p and As-3d as semi-core states, and the lower states as the core states. For the

^a e-mail: bgliu@mail.iphy.ac.cn

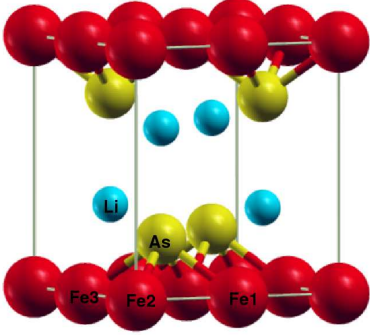


Fig. 1. (color online). Schematic crystal structure of stoichiometric LiFeAs ($P4/nmm$). The biggest ball is Fe atom, the medium As, and the smallest Li.

core states, the full relativistic effect is calculated with radial Dirac equations. For valence and semi-core states, the relativistic effect is calculated under the scalar approximation, with spin-orbit interaction being neglected [39]. We take $R_{\text{mt}} = K_{\text{max}} = 7.5$ and make the angular expansion up to $l = 10$ in the muffin-tin spheres. We use 1000 k points in the first Brillouin zone for different magnetic structures. The self-consistent calculations are controlled by the charge density in real space. The integration of the absolute charge-density difference between two successive self-consistent loops, as the convergence standard, is less than 0.0001 e per unit cell, where e is the electron charge. For all the magnetic structures, we optimize the volume, geometry, and internal position parameters in terms of total energy and the force by the standard 1.5 mRy/a.u.

3 Fully optimized structures with different magnetic orders

Stoichiometric LiFeAs crystallizes into a tetragonal structure with space group $P4/nmm$ at room temperature. As is shown in Fig. 1, its unit cell consists of one Fe-As layer separated by two Li layers. The experimental lattice constants are $a = 3.791 \text{ \AA}$ and $c = 6.364 \text{ \AA}$ [14]. To determine the ground state of LiFeAs , we arrange the Fe moments in the Fe layer so as to form nonmagnetic (NM), ferromagnetic (FM), checkerboard antiferromagnetic (CAF), and SAF orders. In the z direction, the successive Fe layers can couple ferromagnetically or antiferromagnetically. Thus, we have four different AFM orders, namely, CAF-FM, CAF-AFM, SAF-FM and SAF-AFM. Structural optimization is done for these six magnetic orders. Our volume optimization results are presented in Fig. 2. The equilibrium volume is determined by the minimum of the total energy against volume. The optimized results summarized

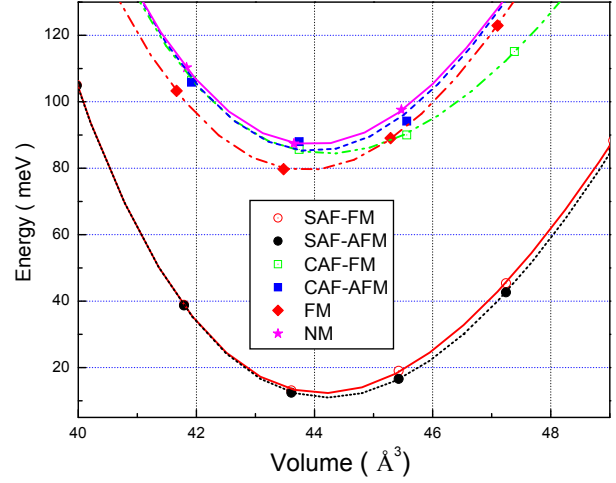


Fig. 2. (color online). The optimization curves of relative total energy (meV) as functions of the volume (\AA^3), per formula unit, for the six possible magnetic orders of stoichiometric LiFeAs .

Table I. The Fe layer in SAF order, either FM or AFM in z direction, is lower than that in other magnetic orders. We conclude that the magnetic ground state of LiFeAs is the magnetic configuration SAF-AFM that the spins in the Fe layers are in the SAF order and the inter-layer magnetic coupling is a weak AFM interaction. This is the same as the magnetic ground states of other FeAs-based parent compounds and tetragonal FeSe [8,12,18,22,23].

The equilibrium volume (88.49 \AA^3) of the ground state is a little smaller than the experimental value (91.46 \AA^3). The magnetic moment per Fe atom is $1.58 \mu_B$. The moment for the CAF order is smaller. For comparison, we do similar calculations using LSDA. The LSDA magnetic moment per Fe atom, $0.62 \mu_B$ and $0.63 \mu_B$ for the SAF-FM and SAF-AFM orders, are much smaller than the GGA results ($1.50 \mu_B$ and $1.58 \mu_B$), respectively. The Fe-As layer, especially the Fe-As distance and the Fe-As-Fe angle, is important for the ground state of LiFeAs . This can be easily seen in Table 1 that as the magnetic moment M of Fe atom increases, the values of the distance $d_{\text{Fe-As}}$ between Fe and As atoms increases and the Fe-As-Fe angles (\angle and \angle) decreased. The trend of M with different $d_{\text{Fe-As}}$ is consistent with previous result calculated with experimental lattice constants [27]. The Fe-As layer as a whole is quite robust and Li atoms are dispersed independently between the Fe-As layers, which explains why we can get exact positions of As atoms (0.2334 compared to the experimental value 0.2365), but a little deviated results for Li atoms (0.3322 to 0.3459). It looks like that the Li atoms play less important roles in the materials.

4 Spin dependent Electronic structures

In the following, we study the electronic properties of stoichiometric LiFeAs in SAF order. The magnetic structure in the Fe layer is shown in Fig. 3 (a). The arrow implies

Table 1. The relative total energy per unit cell (E , with that of the lowest SAF-AFM set to zero), the magnetic moment of Fe atom (M), the equilibrium volume per unit cell (V), the internal position parameters of Li and As (z_{Li} and z_{As}), the distance between Fe and As atoms $d_{\text{Fe-As}}$, two angles formed by Fe1-As-Fe2 (\angle) and Fe1-As-Fe3 (\angle) of LiFeAs in the six possible magnetic orders.

Name	E (meV)	M (μ_B)	V (\AA^3)	z_{Li}	z_{As}	$d_{\text{Fe-As}}$ (\AA)		
FM	140.	0.43	88.47	0.3304	0.2238	2.345	68.8	106.1
NM	151.	{	87.85	0.3313	0.2237	2.339	68.9	106.1
CAF-AFM	151.	1.02	87.83	0.3330	0.2284	2.356	68.4	105.4
CAF-FM	148.	1.18	88.45	0.3330	0.2286	2.362	68.3	105.0
SAF-FM	2.	1.50	88.31	0.3353	0.2324	2.376	67.8	104.0
SAF-AFM	0	1.58	88.49	0.3322	0.2334	2.382	67.6	103.8

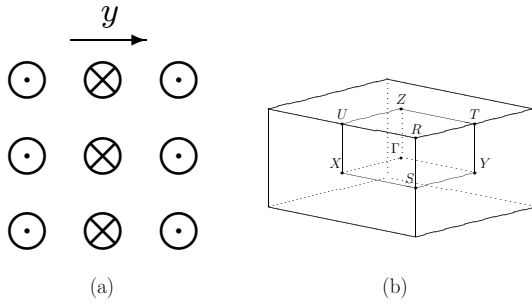


Fig. 3. (a) The magnetic structure of the Fe layer of the LiFeAs ground state, (b) The first Brillouin zone of the LiFeAs ground-state phase with the high-symmetry points labelled.

that the Fe spins align ferromagnetically in the x direction and antiferromagnetically in y direction. Also we show the first Brillouin zone with key representative points and lines emphasized in Fig. 3(b). The total spin-dependent density of states (DOS) and the partial DOSs projected in the mu - n -tin spheres of Fe1, Fe2, Li, and As atoms and in the interstitial region are shown in Fig. 4. There is no energy gap near the Fermi level and then it shows a metal feature. For the SAF order, the spins of Fe1 and Fe2 are antiparallel, it can be easily recognized in DOS. The DOS can be divided into two energy ranges: from -6.0 eV to -3.0 eV and from -3.0 eV to 0 eV (Fermi level). The former consists of Fe-3d and As-4p states forming the Fe-As bond. In the latter range, the Fe-3d states play a key role. It is easily noted that the Li states have very small weight in the energy window. The spin exchange splitting should be mediated by the d-d direct exchange between the nearest Fe atoms and the p-d hybridization between Fe and As.

In Fig. 5 we present the spin-dependent band structure of LiFeAs with Fe1-3d character in SAF order. The plots look like lines, but consist of hollow circles. The circle diameter is proportional to the weight of Fe1-3d states at that k point. Compared with DOS, we can find that 3d states of Fe play a key role for the magnetic structure. It is clear that the bands become narrow along the z direction. It means that the electron structure shows quite strong two-dimensional character. Also, it can be found that there are hole-like (along $-Z$) and electron-like (along Z -U) band sections.

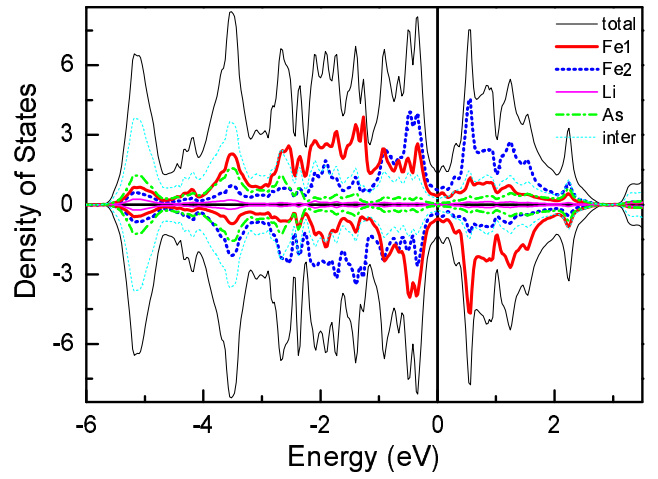


Fig. 4. (color online). Total DOS (states/eV per formula unit) and partial DOS projected in the atomic spheres of Fe1, Fe2, Li, and As and in the interstitial region of the LiFeAs ground-state phase. The upper part is for majority spin and the other for minority spin.

The crystal structures with NM, FM, and CAF orders have the same tetragonal symmetry, while that with SAF is orthorhombic. Different symmetries lead to two different kinds of crystal field splitting for the Fe-3d state. For the tetragonal symmetry, Fe-d state is split into d_{z^2} , d_{xy} , $d_{x^2-y^2}$, and $d_{xz,yz}$, and for orthorhombic symmetry it is split into five singlets. From Fig. 5 we can see that the bands distributions are symmetric along $-X$ and $-Y$ at -3 eV below the Fermi level, but asymmetric near the Fermi level. These are different from the previous NM band structures [8, 27, 34], in which the band distributions are symmetric along $-X$ and $-Y$ for almost all energy range below the Fermi level.

5 Discussions and conclusion

The total energy results, as summarized in Fig. 2 and Table I, show that the magnetic interaction in the z direction is weak, and The SAF structure is lower by 140-151 meV per formula unit than the other magnetic configurations. This is consistent with a simple spin model for the Fe

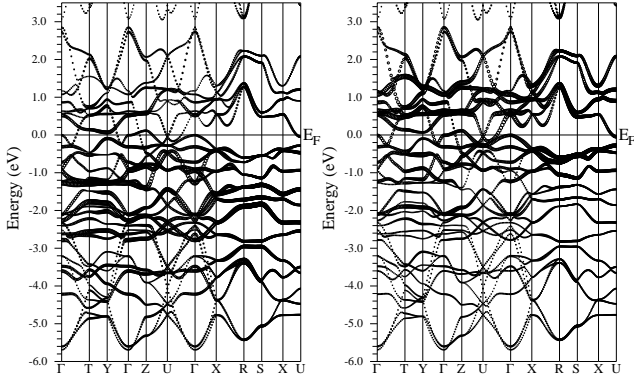


Fig. 5. The spin-dependent energy bands of the LiFeAs ground-state phase. The left part is for majority-spin and the right for minority-spin. The band consists of dots. The bigger the dot is, the more Fe-3d character the band at that point has.

spins, $H = \sum_{ij} J_{ij} S_i \cdot S_j$, where S_i is the spin operator at site i and J_{ij} coupling constants between sites i and j . The summation is limited to the nearest site pairs. J_{ij} is J in the y direction, J in the x direction, and J in the z direction. For such spin model, a non-zero J is necessary to a finite phase transition temperature [40]. The actual J must be tiny because no magnetic phase transition is observed in stoichiometric LiFeAs at any finite temperature.

In summary, we have investigated the structural, electronic, and magnetic properties of stoichiometric LiFeAs by using the density-functional-theory method. We determine the magnetic ground-state by comparing the total energies among all the possible magnetic orders. Our DFT results show the magnetic ground state has the SAF order in the Fe layer and a weak AFM order in the z direction. Our calculated internal positions of Li and As are in good agreement with experiment. Through analyzing electronic and the magnetic results, we propose a simple spin model to understand the experimental magnetic properties. The experimental fact that no magnetic phase transition is observed at finite temperature can be attributed to the tiny inter-layer spin coupling. Thus, we show that stoichiometric LiFeAs has almost the same SAF spin order as other FeAs-based parent compounds and tetragonal FeSe do [8, 12, 18, 22, 23], which may imply that all Fe-based superconductors have the same mechanism of superconductivity.

Acknowledgement. This work is supported by Nature Science Foundation of China (Grant Nos. 10874232 and 10774180), by the Chinese Academy of Sciences (Grant No. KJCX2.YW.W09-5), and by Chinese Department of Science and Technology (Grant No. 2005CB623602).

References

1. Y. Kamihara, T. Watanabe, M. Hirano, and H. Hosono, *J. Am. Chem. Soc.* **130**, 3296 (2008).
2. H. Takahashi, K. Igawa, K. Arii, Y. Kamihara, M. Hirano, and H. Hosono, *Nature* **453**, 376 (2008).

3. X. H. Chen, T. Wu, G. Wu, R. H. Liu, H. Chen, and D. F. Fang, *Nature* **453**, 761 (2008).
4. Z. A. Ren, W. Lu, J. Yang, W. Yi, X. L. Shen, Z. C. Li, G. C. Che, X. L. Dong, L. L. Sun, F. Zhou, and Z. X. Zhao, *Chin. Phys. Lett.* **25**, 2215 (2008).
5. Q. Huang, Y. Qiu, W. Bao, M. A. Green, J. W. Lynn, Y. C. Gasparovic, T. Wu, G. Wu, and X. H. Chen, *Phys. Rev. Lett.* **101**, 257003 (2008).
6. J. Zhao, W. Ratcliff, J. W. Lynn, G. F. Chen, J. L. Luo, N. L. Wang, J. Hu, and P. Dai, *Phys. Rev. B* **78**, 140504(R) (2008).
7. A. I. Goldman, D. N. Argyriou, B. Ouladdiaf, T. Chatterji, A. Kreyssig, S. Nandi, N. Ni, S. L. Bud'ko, P. C. Canfield, and R. J. McQueeney, *Phys. Rev. B* **78**, 100506(R) (2008).
8. D. J. Singh, *Phys. Rev. B* **78**, 094511 (2008).
9. S. Matsushita, Y. Inoue, T. Nomura, M. Hirano, and H. Hosono, *J. Phys. Soc. Jpn.* **77**, 113709 (2008).
10. G. Wu, Y. L. Xie, H. Chen, M. Zhong, R. H. Liu, B. C. Shi, Q. J. Li, X. F. Wang, T. Wu, Y. J. Yan, J. J. Ying and X. H. Chen, *J. Phys.: Condens. Matter* **21**, 142203 (2008).
11. X. Zhu, F. Han, P. Cheng, G. Mu, B. Shen, L. Fang and H. H. Wen, *EPL* **85**, 17011 (2008).
12. L. F. Zhu, and B. G. Liu, *EPL* **85**, 67009 (2009).
13. X. C. Wang, Q. Q. Liu, Y. X. Lv, W. B. Gao, L. X. Yang, R. C. Yu, F. Y. Li, and C. Q. Jin, *Solid State Commun.* **148**, 538 (2008).
14. J. H. Tapp, Z. Tang, B. Lv, K. Sasmal, B. Lorenz, P. C. Wu, Chu, and A. M. Gulby, *Phys. Rev. B* **78**, 060505(R) (2008).
15. M. J. Pitcher, D. R. Parker, P. Adamson, S. J. C. Herklrath, A. T. Boothroyd, R. M. Ibberson, M. Brunelli, and S. J. Clarke, *Chem. Commun.* **2008**, 5918 (2008).
16. Y. Mizuguchi, F. Tomioka, S. Tsuda, T. Yamaguchi and Y. Takano, *Appl. Phys. Lett.*, **93**, 152505 (2008).
17. J. Zhang, D. J. Singh, and M. H. Du, *Phys. Rev. B*, **78**, 134514 (2008).
18. Y. F. Li, L. F. Zhu, S. D. Guo, Y. C. Xu, and B. G. Liu, *J. Phys.: Condens. Matter*, **21**, 115701 (2009).
19. F. C. Hsu, J. Y. Luo, K. W. Yeh, T. K. Chen, T. W. Huang, P. M. Wu, Y. C. Lee, Y. L. Huang, Y. Y. Chu, D. C. Yan, and M. K. Wu, *Proc. Natl. Acad. Sci. USA*, **105**, 14262 (2008).
20. C. de la Cruz, Q. Huang, J. W. Lynn, J. Li, W. R. Ratcliff, J. L. Zarestky, H. A. Mook, G. F. Chen, J. L. Luo, N. L. Wang, and P. Dai, *Nature* **453**, 899 (2008).
21. S. Ishibashi, K. Terakura, and H. Hosono, *J. Phys. Soc. Japan* **77**, 053709 (2008).
22. Z. P. Yin, S. Lebegue, M. J. Han, B. P. Neal, S. Y. Savrasov, and W. E. Pickett, *Phys. Rev. Lett.* **101**, 047001 (2008).
23. T. Yildirim, *Phys. Rev. Lett.* **101**, 057010 (2008).
24. D. J. Singh, and M. H. Du, *Phys. Rev. Lett.* **100**, 237003 (2008).
25. I. I. Mazin, D. J. Singh, M. D. Johannes, and M. H. Du, *Phys. Rev. Lett.* **101**, 057003 (2008).
26. A. S. Sefat, M. A. McGuire, B. C. Sales, R. Jin, J. Y. Howe, and D. Mandrus, *Phys. Rev. B* **77**, 174503 (2008).
27. K. D. Belashchenko and V. P. Antropov, *Phys. Rev. B* **78**, 212505 (2008).
28. F. L. Pratt, P. J. Baker, S. J. Blundell, T. Lancaster, H. J. Lewtas, P. Adamson, M. J. Pitcher, D. R. Parker, and S. J. Clarke, *arXiv:0810.0973* (2008).
29. M. Mito, M. J. Pitcher, W. Crichton, G. Garbarino, P. J. Baker, S. J. Blundell, P. Adamson, D. R. Parker, and S. J. Clarke, *J. Am. Chem. Soc.* **131**, 2986 (2009).

30. M. G. Goch, B. Lv, J. H. Tapp, Z. Tang, B. Lorenz, A. M. Guly, and P. C. W. Chu, *EPL* 85, 27005 (2009).
31. S. Li, C. de la Cruz, Q. Huang, G. F. Chen, T.-L. Xia, J. L. Lou, N. L. Wang, and P. Dai, *arXiv*:0903.0525 (2009).
32. E. Z. Kumeau, J. M. Cleod, N. A. Skorikov, L. D. Finkelstein, A. M. Oeves, M. A. Korotin, Y. A. Izyumov, and S. Clarke, *arXiv*:0903.4901 (2009).
33. C. W. Chu, F. Chen, M. Goch, A. M. Guly, B. Lorenz, B. Lv, K. Sasmal, Z. J. Tang, J. H. Tapp, and Y. Y. Xue, *arXiv*:0902.0806 (2009).
34. I. A. Nekrasov, Z. V. Pchelkina, and M. V. Sadovskii, *JETP Lett.* 88, 543 (2008).
35. P. Hohenberg and W. Kohn, *Phys. Rev.* 136, B864 (1964); W. Kohn and L. J. Sham, *Phys. Rev.* 140, A1133 (1965).
36. P. Blaha, K. Schwarz, P. Sorantin, and S. B. Trickey, *Comput. Phys. Commun.* 59, 399 (1990).
37. P. Blaha, K. Schwarz, G. K. H. Madsen, D. Kvasnicka, and J. Luitz, *WIEN 2k* (K. Schwarz, Tech. Univ. Wien, Austria) (2001), ISBN 3-9501031-1-2.
38. J. P. Perdew, K. Burke, and M. Ernzerhof, *Phys. Rev. Lett.* 77, 3865 (1996).
39. D. D. Koelling and B. N. Harmon, *J. Phys. C* 10, 3107 (1977); D. Singh, *Planewaves, pseudopotentials and the LAPW method*, Kluwer Academic 1994.
40. B.-G. Liu, *Phys. Rev. B* 41, 9563 (1990); G.-B. Liu and B.-G. Liu, *J. Phys.: Condens. Matter* 21, 195701 (2009).